Chemical Engineering Journal 151 (2009) 46–50

Contents lists available at ScienceDirect

Chemical Engineering Journal

journal homepage: www.elsevier.com/locate/cej

Photodegradation of carboxylic acids on Pr_6O_{11} surface. Enhancement by semiconductors

C. Karunakaran*, R. Dhanalakshmi, P. Anilkumar

Department of Chemistry, Annamalai University, Annamalainagar 608002, Tamilnadu, India

ARTICLE INFO

Article history:
Received 28 October 2008
Received in revised form 19 January 2009
Accepted 26 January 2009

Keywords:
Insulator
Semiconductor
Interparticle charge-transfer
Photocatalysis

ABSTRACT

Oxalic acid is photooxidized on Pr_6O_{11} surface under UV-A light and the reaction follows first-order kinetics with a linear dependence on the photon flux. The photonic efficiency is higher with UV-C light than with UV-A light. While TiO_2, ZnO, CuO, Bi_2O_3, and Nb_2O_5 individually photocatalyze the oxidation, each semiconductor, when present along with Pr_6O_{11}, shows enhanced oxidation indicating interparticle hole-jump from the band gap-excited semiconductor to oxalic acid-adsorbed on Pr_6O_{11}. The photonic efficiency of the oxidation on Pr_6O_{11} surface is of the order: formic acid > oxalic acid > acetic acid; citric acid is unsusceptible to oxidation.

1. Introduction

Band gap-illumination of semiconductors creates electron–hole pairs, holes in the valence band and electrons in the conduction band [1]. A fraction of these pairs diffuses out to the surface of the crystal and takes part in chemical reactions with adsorbed electron donors and acceptors, resulting in photocatalysis. While the hole oxidizes the organics the electron is taken up by the adsorbed oxygen molecule, yielding highly unstable superoxide radical, $O_2^{\bullet -}$ [2]. In aqueous medium, $O_2^{\bullet -}$ in turn generates reactive species such as $HO^{\bullet}$, $HO_2^{\bullet}$, and H_2O_2, which also oxidize the organics. Water is adsorbed on the surface of semiconductor, both molecularly and dissociatively [3,4]. Hole-trapping by either the surface hydroxyl groups or adsorbed water molecules results in short-lived $HO^{\bullet}$ radicals, which are the primary oxidizing agents [5–8]. Semiconductor-photocatalysis is of interest due to its application in environmental remediation. But what we report here is photooxidation on the surface of Pr_6O_{11}, an insulator; the widely investigated mineralization of oxalic acid is the test reaction taken up for the detailed study [9–15]. In the presence of air, oxalic acid undergoes clean photomineralization without the formation of any long-lived intermediates and earlier workers have followed the reaction by measuring the CO_2-liberation also [14]. Coupling two different semiconductors enables a vectorial transfer of electron and hole from one semiconductor to another. Under band gap-illumination, the semiconductors are simultaneously activated. While the electrons accumulate at the lower-lying conduction band of one semiconductor, the holes migrate to the less anodic valence band. These processes of charge separation are very fast. Improved charge separation increases the efficiency of reduction or oxidation of the adsorbed substrate. Reports on interparticle charge-transfer between semiconductors are many. While a couple of studies are on charge-transfer between two particulate semiconductors [16,17], the others deal with coupled semiconductors [18,19]. But, our results reveal that the oxalic acid oxidation on Pr_6O_{11} is enhanced by semiconductors, an unusual synergism when a semiconductor is present along with an insulator.

2. Experimental

2.1. Materials

Pr_6O_{11} (Sd fine), TiO_2 (Merck), ZnO (Merck), CuO (Sd fine), Bi_2O_3 (Sd fine), Nb_2O_5 (Sd fine), and Al_2O_3 (Merck) were of analytical grade and used as received.

2.2. Photoreactors

The photooxidation was studied in a multilamp-photoreactor fitted with eight 8 W mercury lamps of wavelength 365 nm (Sankyo Denki, Japan), a highly polished anodized aluminum reflector and four cooling fans. The reaction vessel was a borosilicate glass tube of 15 mm inner diameter, placed at the centre. The light intensity was adjusted by employing two, four, and eight lamps, with the angle sustained by the adjacent lamps at the sample as 180°, 90°, and 45°, respectively. The oxidation was also studied in a micro-photoreactor fitted with a 6 W 254 nm low-pressure mercury

* Corresponding author. Tel.: +91 9443481590; fax: +91 4144238145.
E-mail address: karunakaranc@rediffmail.com (C. Karunakaran).

1385-8947/$ – see front matter © 2009 Elsevier B.V. All rights reserved.
doi:10.1016/j.cej.2009.01.042

lamp and a 6 W 365 nm mercury lamp. Quartz and borosilicate glass tubes were used for 254 and 365 nm lamps, respectively. The photon flux (I) under each experimental condition was determined by ferrioxalate actinometry [20].

2.3. Method

The photooxidation was carried out with 25 and 10 mL of oxalic acid solutions in the multilamp and micro-photoreactors, respectively. The solutions were continuously purged with air, which effectively kept the added catalyst under suspension and at constant motion. The airflow rate was determined by the soap bubble method. After illumination, the catalyst was recovered by centrifugation and the leftover oxalic acid was analyzed by alkalimetry and also by permanganometry [9,21]. Both the results were identical. The decrease in acid concentration for a finite time of illumination afforded the reaction rate, which was reproducible to ±5%. A time lag of at least 15 min was provided prior to illumination to ensure pre-adsorption of the acid on the oxide. The dissolved O_2 was determined using an Elico dissolved oxygen analyzer PE 135. An Avatar 330FT-IR spectrometer was used to record the infrared spectra and the diffuse reflectance spectra were obtained using Shimadzu UV-2450 UV–visible spectrometer with $BaSO_4$ as the reference. Pre-sonication was made with Toshcon SW 2 ultrasonic bath (37 ± 3 kHz, 150 W).

3. Results and discussion

3.1. Catalysts characterization

The TiO_2 employed is of anatase phase; the X-ray diffraction pattern of the sample is identical with the standard pattern of anatase (JCPDS 00-021-1272) and the rutile lines (00-034-0180 D) are absent (Siemens D-5000 XRD, Cu Kα X-ray, λ = 1.54 Å, scan: 5–60°, scan speed: 0.2° s^{-1}). The diffraction of ZnO is that of the JCPDS pattern of zincite (00-005-0664 D; Bruker D8 XRD, Cu Kα X-ray, λ = 1.5406 Å, scan: 5–70°, scan speed: 0.050° s^{-1}). The XRD of Al_2O_3 matches with the standard JCPDS patterns of γ-Al_2O_3 (00-001-1308 D, cubic: a: 7.900 Å, b: 7.900 Å, c: 7.900 Å, α: 90.0°, β: 90.0°, γ: 90.0°) and χ-Al_2O_3 (00-004-0880 N, cubic: a: 7.950 Å, b: 7.950 Å, c: 7.950 Å, α: 90.0°, β: 90.0°, γ: 90.0°), revealing the presence of both the phases (γ:χ::52:48). The particle sizes were measured using particle sizer Horiba LA-910 or Malvern 3600E (focal length 100 mm, beam length 2.0 mm, wet (methanol) presentation) as follows: Pr_6O_{11}: 3.03–8.89 μm, TiO_2: 2.6–27.6 μm, ZnO: 3.5–27.6 μm, CuO: 5.69–30.5 μm, Bi_2O_3: 0.17–0.49 μm, Nb_2O_5: 0.22–0.43 μm, Al_2O_3: 2.6–57.7 μm. The BET surface areas were determined as below: TiO_2: 14.68 m^2 g^{-1}, ZnO: 12.16 m^2 g^{-1}, CuO: 1.51 m^2 g^{-1}, Bi_2O_3: 2.75 m^2 g^{-1}, Nb_2O_5: 1.94 m^2 g^{-1}, Al_2O_3: 10.63 m^2 g^{-1}.

3.2. Photooxidation on Pr_6O_{11}

In the presence of air, oxalic acid is photooxidized on the surface of Pr_6O_{11} and the influence of operational parameters like oxalic acid concentration, catalyst loading and light intensity on the oxidation has been studied using the multilamp-photoreactor with mercury lamps of wavelength 365 nm. Oxalic acid gets adsorbed over Pr_6O_{11}. The infrared spectrum of Pr_6O_{11}, recovered from the oxalic acid solution prior to illumination and dried at 100 °C, reveals characteristic absorbance around 1640 and 3440 cm^{-1}. The adsorption of oxalic acid (25 mL 1.0 M) on Pr_6O_{11} (0.050 g) is 4% while the photooxidation in 30 min at 25.4 μEinstein L^{-1} s^{-1} is 44% (7.8 mL s^{-1} airflow, 24.7 mg L^{-1} dissolved O_2, 365 nm). The oxidation of oxalic acid in the absence of Pr_6O_{11} is insignificant. Also, there is no loss of oxalic acid due to purging of air. Fig. 1 is a temporal profile of oxalic acid oxidation on Pr_6O_{11}. The Pr_6O_{11} surface shows sustainable activity. The recycled Pr_6O_{11} without any pre-treatment provides identical photooxidation results. The measurement of the oxidation rates at different oxalic acid concentrations shows linear increase of the reaction rate with oxalic acid concentration and Fig. 2 reveals the first-order kinetics. Also, as shown in Fig. 3, the photooxidation rate increases linearly with the photon flux; the loss of oxalic acid due to photolysis is small. The photonic efficiency of oxidation is moderately enhanced by increasing the catalyst loading. Doubling the catalyst loading from 0.05 to 0.10 g improves the photonic efficiency from 49 to 58% (Table 1, Fig. 4). Investigation of the reaction using a 6 W 365 nm mercury lamp and a 6 W 254 nm low-pressure mercury lamp, separately in the micro-reactor under identical conditions, shows that UV-C light is more effective than UV-A light to oxidize oxalic acid. The photonic efficiencies of the oxidation with

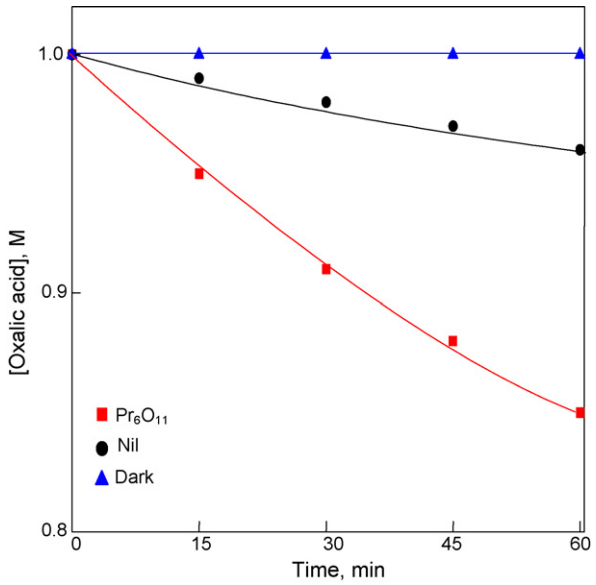

Fig. 1. Temporal profile of the photodegradation of oxalic acid on Pr_6O_{11}. 0.050 g Pr_6O_{11} loading, 7.8 mL s^{-1} airflow rate, 24.7 mg L^{-1} dissolved O_2, 365 nm, 14.0 μEinstein L^{-1} s^{-1}, 25 mL oxalic acid.

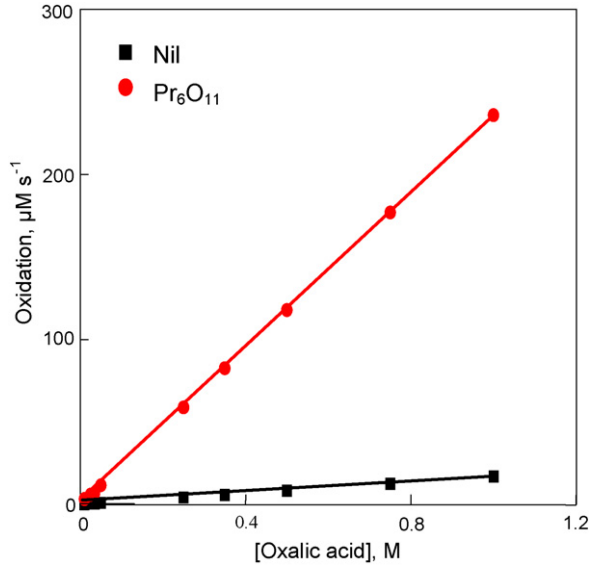

Fig. 2. Photodegradation as a function of concentration. 0.050 g Pr_6O_{11} loading, 7.8 mL s^{-1} airflow rate, 24.7 mg L^{-1} dissolved O_2, 365 nm, 25.4 μEinstein L^{-1} s^{-1}, 25 mL oxalic acid.

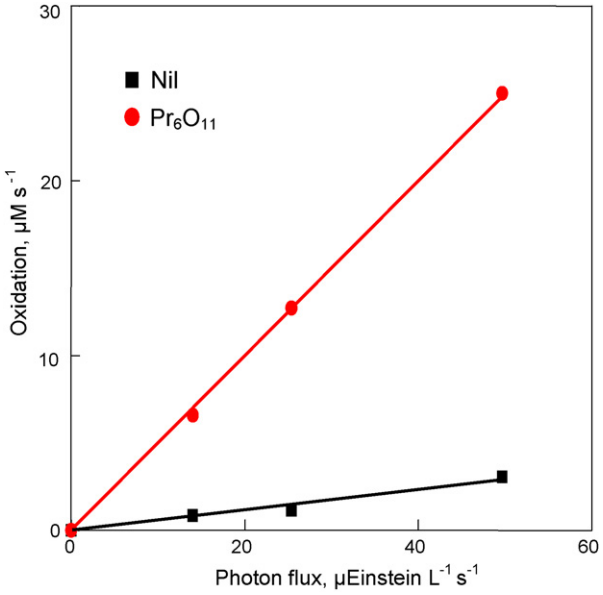

Fig. 3. Photodegradation as a function of photon flux. 25 mL 0.050 M oxalic acid, 0.050 g Pr_6O_{11} loading, 7.8 mL s^{-1} airflow rate, 24.7 mg L^{-1} dissolved O_2, 365 nm.

Table 1
The photonic efficiencies (%ξ) of oxalic acid degradation[a].

Catalyst loading (g)	%ξ					
	TiO_2	ZnO	CuO	Bi_2O_3	Nb_2O_5	Pr_6O_{11}
0.05	39	54	24	22	45	49
0.10	47	66	38	32	52	58

[a] 25 mL 0.050 M oxalic acid, 7.8 mL s^{-1} airflow rate, 24.7 mg L^{-1} dissolved O_2, 365 nm, 24.7 μEinstein L^{-1} s^{-1}, 10 min illumination.

light of 365 and 254 nm are 66 and 77%, respectively (10 mL 0.050 M oxalic acid, 0.050 g Pr_6O_{11} loading, 7.8 mL s^{-1} airflow rate, 24.7 mg L^{-1} dissolved O_2). Dissolved O_2 is required for the reaction and deaeration of oxalic acid solution by purging N_2 instead of air arrests the oxidation (conditions as in Table 1 with 0.05 g Pr_6O_{11} loading and 3.3 and 24.7 mg L^{-1} of dissolved O_2 in N_2- and air-purged solutions, respectively). Anions like Cl^-, Br^-, SO_4^{2-}, and NO_3^- do not interfere in the photoprocess. Addition of the

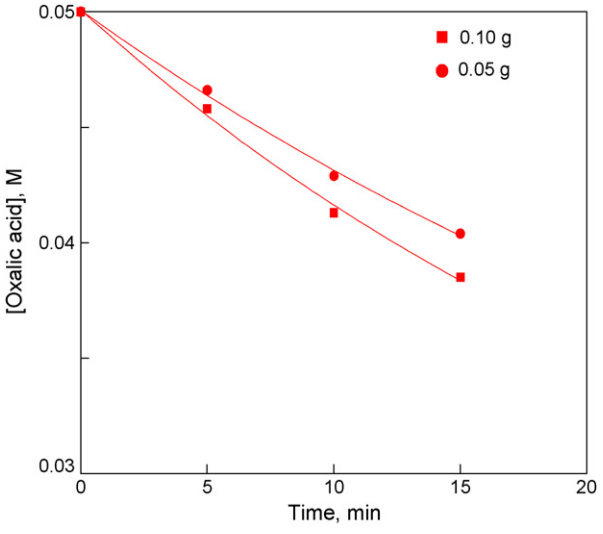

Fig. 4. Photodegradation at different Pr_6O_{11} loading, 7.8 mL s^{-1} airflow rate, 24.7 mg L^{-1} dissolved O_2, 365 nm, 24.7 μEinstein L^{-1} s^{-1}, 25 mL oxalic acid.

corresponding potassium salts (0.10 mM), under the conditions stated in Table 1 with 0.050 g of Pr_6O_{11} loading, does not alter the photonic efficiency remarkably. Further, under the stated experimental conditions, vinyl monomers like acrylonitrile and acryl amide (5 mM) neither suppress the photonic efficiency nor get polymerized indicating the absence of a chain carrier in the solution phase. Anionic as well as cationic micelles like aerosol OT, sodium lauryl sulfate and cetyltrimethylammonium bromide (5 mM) do not suppress the photonic efficiency suggesting that the photooxidation rate is not determined by reaction in solution, if any; the experimental condition remains the same. Under the same reaction conditions, singlet O_2 quencher azide ion (0.10 mM) fails to inhibit the oxidation indicating the absence of the involvement of $^1O_2$ in the photoprocess. Generally, the photocatalytic activity is susceptible to the surface and size modification of the catalyst particles. Sonication in aqueous solution causes rapid formation, growth and collapse of cavities resulting in local high pressures and temperatures, which are responsible for surface and particle size modification of the catalyst [22]. However, pre-sonication does not change the activity of Pr_6O_{11} surface; the oxalic acid oxidation rate on Pr_6O_{11} surface is not significantly altered by pre-sonication for 10 min at 37 ± 3 kHz and 150 W; the experimental conditions are as stated earlier. While oxalic acid is easily photooxidized oxalate ion resists the same. Under the conditions given in Table 1 with 0.050 g Pr_6O_{11} loading, the photonic efficiency of the oxidation of oxalate ion (0.05 M) is 8% while that of oxalic acid is 49%. This suggests that it is the undissociated oxalic acid molecule but not the oxalate anion that gets adsorbed over Pr_6O_{11} surface and undergoes oxidation.

3.3. Mechanism

Oxalic acid is adsorbed on Pr_6O_{11}. The acidic sites on the surface of Pr_6O_{11} may coordinate with the carbonyl oxygen and/or the basic O^- group may be involved in hydrogen bonding with the –OH group of the carboxylic acid. The possible mechanism is the absorption of light by oxalic acid molecule adsorbed on Pr_6O_{11} resulting in its excitation. The diffuse reflectance spectra of oxalic acid-adsorbed Pr_6O_{11} and bare Pr_6O_{11} confirm the same. While oxalic acid-adsorbed Pr_6O_{11} absorbs light at the wavelength of illumination, the bare Pr_6O_{11} does not (Fig. 5). Transfer of the excited electron to a neighboring adsorbed O_2 molecule may initiate the degradation of oxalic acid. The suggested mechanism is supported by the report that 2,4,5-trichlorophenol forms a charge-transfer complex with TiO_2 which is activated by light of wavelength as long as 520 nm resulting in photochemical reaction [23]. The fact that the reaction on Pr_6O_{11} surface does not occur in the absence of oxygen is in agreement with the suggested mechanism.

3.4. Kinetic law

The Langmuir–Hinshelwood kinetic law is applicable to photooxidation and hence [24]:

$$\text{rate} = \frac{kK_1K_2ICS[\text{acid}][O_2]}{(1+K_1[\text{acid}])(1+K_2[O_2])}$$

where K_1 and K_2 are the adsorption coefficients of oxalic acid and O_2 on the illuminated Pr_6O_{11} surface, k is the specific oxidation rate, S is the specific surface area of Pr_6O_{11}, C is Pr_6O_{11} loading per litre and I is the light intensity in Einstein L^{-1} s^{-1}. The acid solution was oxygen-saturated by continuous purging of air and hence the dissolved oxygen concentration remained constant during the photooxidation. Since K_2 is constant $K_2[O_2]/(1+K_2[O_2])$ is also a constant. The Langmuir–Hinshelwood kinetic law is valid for the observed results provided the adsorption coefficient of the acid on the illuminated Pr_6O_{11} surface (K_1) is small so that $1 \gg K_1[\text{acid}]$. This

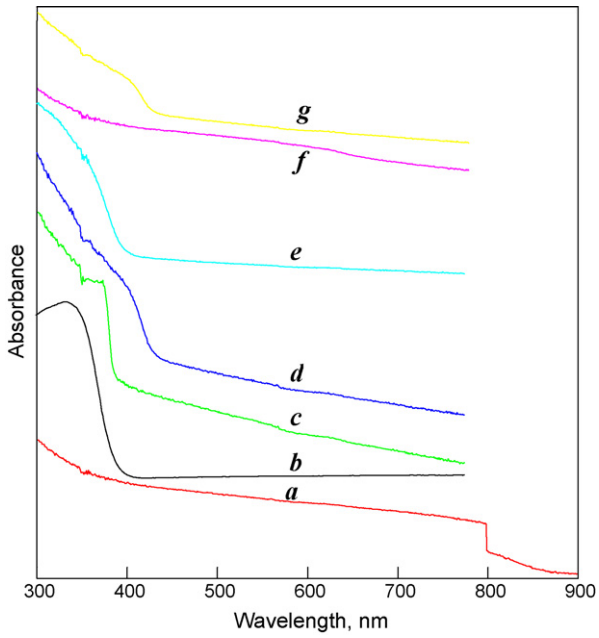

Fig. 5. Diffuse reflectance spectra, (a) CuO, (b) TiO_2, (c) ZnO, (d) Bi_2O_3, (e) Nb_2O_5, (f) Pr_6O_{11}, and (g) oxalic acid-adsorbed Pr_6O_{11}.

simplifies the Langmuir–Hinshelwood equation to a linear dependence of the oxidation rate on the acid concentration.

3.5. Semiconductor-photocatalysis

TiO_2, ZnO, CuO, Bi_2O_3, and Nb_2O_5 photocatalyze the oxidation of oxalic acid. Table 1 presents the photonic efficiencies of these oxides and the corresponding values of Pr_6O_{11} are also appended for comparison. The semiconductors exhibit band gap-excitation under UV-A light, as seen from their diffuse reflectance spectra (Fig. 5). Hence the mechanism of the photooxidation of oxalic acid on these semiconductors is that through the band gap-excitation, which has been discussed elsewhere [9]. As expected, under identical experimental conditions Al_2O_3, an insulator, does not catalyze the photooxidation of oxalic acid.

3.6. Synergism by semiconductors

Band gap-illumination of semiconductors in a mixture enables vectorial transfer of holes and excited electrons from one semiconductor to another resulting in improved photocatalytic efficiency and enhanced photocatalysis by semiconductor mixtures is known [16,17]. But what we report here is enhanced photocatalysis due to the presence of a particulate semiconductor with particulate Pr_6O_{11}, both under suspension and at continuous motion. All the semiconductors used show the enhancement with Pr_6O_{11} (Fig. 6). This is because of hole-transfer from the band gap-excited semiconductor to the oxalic acid molecule adsorbed on Pr_6O_{11}.

3.7. Ease of oxidation of carboxylic acids on Pr_6O_{11}

Pr_6O_{11} also mediates the oxidation of formic and acetic acids under UV-A light but fails in the case of citric acid. Table 2 presents the photonic efficiencies of degradation of formic, oxalic, acetic and citric acids. The ease of oxidation is as follows: formic acid > oxalic acid > acetic acid. This order is in agreement with those observed on TiO_2, ZnO, CuO, and Bi_2O_3 surfaces under natural sunlight [9]. However, these semiconductors also catalyze the degradation of citric acid under solar radiation, although less efficiently.

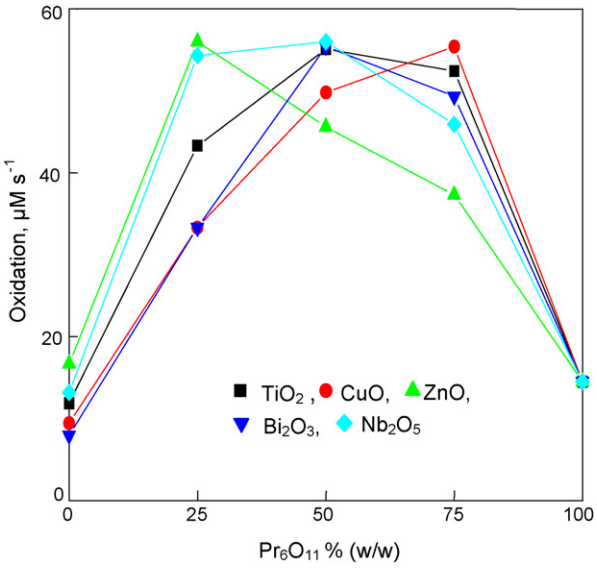

Fig. 6. Enhanced oxidation on Pr_6O_{11} with semiconductors, 25 mL 0.050 M oxalic acid, 0.10 g total catalyst loading, 7.8 mL s^{-1} airflow rate, 24.7 mg L^{-1} dissolved O_2, 365 nm, 25.4 μEinstein L^{-1} s^{-1}.

Table 2
Photonic efficiencies (%ξ) of degradation of carboxylic acids on Pr_6O_{11}[a].

Acid	%ξ
Formic	93
Oxalic	49
Acetic	28
Citric	0

[a] 25 mL 0.050 M acid, 0.050 g Pr_6O_{11} loading, 7.8 mL s^{-1} airflow rate, 24.7 mg L^{-1} dissolved O_2, 365 nm, 24.7 μEinstein L^{-1} s^{-1}, 10 min illumination.

4. Conclusions

Pr_6O_{11} mediates the oxidation of oxalic acid under UV-A light and the photonic efficiency is larger with UV-C light. The oxidation follows first-order kinetics and exhibits linear dependence on the light intensity. TiO_2, ZnO, CuO, Bi_2O_3, and Nb_2O_5 individually photocatalyze the oxidation of oxalic acid and with Pr_6O_{11} they show synergism, an enhanced oxalic acid-photooxidation, implying electron-transfer from the oxalic acid-adsorbed on Pr_6O_{11} to the illuminated semiconductor during collision. The photonic efficiency of oxidation on Pr_6O_{11} surface is of the order: formic acid > oxalic acid > acetic acid; citric acid fails to degrade.

Acknowledgements

The authors thank the Council of Scientific and Industrial Research (CSIR), New Delhi, for the financial support through research Grant no. 01(2031)/06/EMR-II and RD is grateful to Annamalai University for UF.

References

[1] M.R. Hoffmann, S.T. Martin, W. Choi, D.W. Bahnemann, Environmental applications of semiconductor photocatalysis, Chem. Rev. 95 (1995) 69–96.
[2] T.L. Thompson, J.T. Yates Jr., Surface science studies of the photoactivation of TiO_2—new photochemical process, Chem. Rev. 106 (2006) 4428–4453.
[3] R. Osgood, Photoreaction dynamics of molecular adsorbates on semiconductor and oxide surfaces, Chem. Rev. 106 (2006) 4379–4401.
[4] J. Zhao, B. Li, K. Onda, M. Feng, H. Petek, Solvated electrons on metal oxide surfaces, Chem. Rev. 106 (2006) 4402–4427.
[5] J. Peller, O. Wiest, P.V. Kamat, Hydroxy radical's role in the remediation of a common herbicide, 2,4-dichlorophenoxyacetic acid (2,4-D), J. Phys. Chem. A 108 (2004) 10925–10933.

[6] Y. Shiraishi, N. Saito, T. Hirai, Adsorption-driven photocatalytic activity of mesoporous titanium dioxide, J. Am. Chem. Soc. 127 (2005) 12820–12822.
[7] Y. Du, J. Rabani, The measure of TiO_2 photocatalytic efficiency and the comparison of different photocatalytic titania, J. Phys. Chem. B 107 (2003) 11970–11978.
[8] L. Sun, J.R. Bolton, Determination of the quantum yield for the photochemical generation of hydroxyl radicals in TiO_2 suspensions, J. Phys. Chem. 100 (1996) 4127–4134.
[9] C. Karunakaran, R. Dhanalakshmi, Photocatalytic performance of particulate semiconductors under natural sunshine—oxidation of carboxylic acids, Sol. Energy Mater. Sol. Cells 92 (2008) 588–593.
[10] W.Y. Teoh, R. Amal, L. Madler, S.E. Pratsinis, Flame sprayed visible light-active Fe–TiO_2 for photomineralization of oxalic acid, Catal. Today 120 (2007) 203–213.
[11] V. Iliev, D. Tomova, L. Bilyarska, G. Tyuliev, Influence of the size of gold nanoparticles deposited on TiO_2 upon the photocatalytic destruction of oxalic acid, J. Mol. Catal. A 263 (2007) 32–38.
[12] V. Iliev, D. Tomova, L. Bilyarska, A. Eliyas, L. Petrov, Photocatalytic properties of TiO_2 modified with platinum and silver nanoparticles in the degradation of oxalic acid in aqueous solution, Appl. Catal. B 63 (2006) 266–271.
[13] M.I. Franch, J.A. Ayllon, J. Peral, X. Domenech, Photocatalytic degradation of short-chain organic diacids, Catal. Today 76 (2002) 221–233.
[14] M.M. Kosanic, Photocatalytic degradation of oxalic acid over TiO_2 powder, J. Photochem. Photobiol. A 119 (1998) 119–122.
[15] K. Kobayakawa, C. Sato, Y. Sato, A. Fujishima, Continuous-flow photoreactor packed with titanium dioxide immobilized on large silica gel beads to decompose oxalic acid in excess water, J. Photochem. Photobiol. A 118 (1998) 65–69.
[16] N. Serpone, P. Maruthamuthu, P. Pichat, E. Pelizzetti, H. Hidaka, Exploiting the interparticle electron transfer process in the photocatalyzed oxidation of phenol, 2-chlorophenol and pentachlorophenol: chemical evidence for electron and hole transfer between coupled semiconductors, J. Photochem. Photobiol. A 85 (1995) 247–255.
[17] N. Serpone, E. Borgarello, M. Gratzel, Visible light induced generation of hydrogen from H_2S in mixed semiconductor dispersions: improved efficiency through inter-particle electron transfer, J. Chem. Soc. Chem. Commun. (1984) 342–344.
[18] K.C. Kim, C.S. Han, Photocatalysis over titania on iron oxide, J. Phys. IV France 132 (2006) 185–188.
[19] J. Bandara, K. Tennakone, P. Binduhewa, Probing the tunneling of electrons from SnO_2 to ZnO in dye sensitization of composite SnO_2/ZnO by use of generated H_2O_2 via reduction of O_2, New J. Chem. 25 (2001) 1302–1305.
[20] H.J. Kuhn, S.E. Braslavsky, R. Schmidt, Chemical actinometry (IUPAC technical report), Pure Appl. Chem. 76 (2004) 2105–2146.
[21] E. Szabo-Bardos, H. Czili, A. Horvath, Photocatalytic oxidation of oxalic acid enhanced by silver deposition on a TiO_2 surface, J. Photochem. Photobiol. A 154 (2003) 195–201.
[22] K. Hirano, H. Nitta, K. Sawada, Effect of sonication on the photocatalytic mineralization of some chlorinated organic compounds, Ultrason. Sonochem. 12 (2005) 271–276.
[23] A.G. Agrios, K.A. Gray, E. Weitz, Photocatalytic transformation of 2,4,5-trichlorophenol on TiO_2 under sub-band-gap illumination, Langmuir 19 (2003) 1402–1409.
[24] C. Karunakaran, R. Dhanalakshmi, Semiconductor-catalyzed degradation of phenols with sunlight, Sol. Energy Mater. Sol. Cells 92 (2008) 1315–1321.